

# Field-Line Resonances Triggered by a Northward IMF Turning

H. Laakso,<sup>1</sup> D. H. Fairfield,<sup>2</sup> C. T. Russell,<sup>3</sup> J. H. Clemmons,<sup>4</sup> H. J. Singer,<sup>5</sup> B. L. Giles,<sup>6</sup> R. P. Lepping,<sup>2</sup> F. S. Mozer,<sup>7</sup> R. F. Pfaff,<sup>2</sup> K. Tsuruda,<sup>8</sup> and J. R. Wygant<sup>9</sup>

**Abstract.** A sudden northward rotation of the IMF observed by IMP 8 near the bow shock at 21:22 UT on January 10, 1997, triggered surface waves and fast mode waves at the flanks of the duskside magnetosphere, as observed by GEOTAIL instruments. The power spectral density of these waves peaked in the frequency range where field-line resonances were observed by the POLAR satellite in the region  $L = 6.6$ – $10.2$ . The oscillation periods of the observed field-line resonances were  $L$ -dependent with two distinct peaks which may be explained by increased heavy ion content at those field lines. The ULF waves also caused enhanced low-energy ion fluxes from the ionosphere.

## Introduction

Field-line resonances (FLRs) are standing modes of the Earth's dipole magnetic field lines, and their polarization properties depend on local time and  $L$  shell [Samson *et al.*, 1971; Hughes, 1994]. The FLRs are usually quite narrow in the radial direction while a large part of an  $L$  shell can oscillate azimuthally. This is a toroidal resonance mode with an azimuthal magnetic field component and a radial electric field component, commonly observed at geosynchronous distances [Laakso and Schmidt, 1989].

A well-known driver of an FLR is a fast mode wave which is coupled to a shear Alfvén wave at a certain resonant  $L$  shell [Southwood, 1974; Singer *et al.*, 1982]. There is a variety of energy sources that can produce fast mode waves in the magnetosphere. It has been suggested that a major source is the Kelvin-Helmholtz (K-H) instability which can produce surface waves along the magnetopause and emit fast mode waves into the magnetosphere [Pu and Kivelson, 1983]. The orientation of the magnetic field with respect to the surface can play an important role in switching on the K-H instability [Miura, 1995b]. As a consequence of this instability, large-scale vortices are formed in the flanks of the magnetosphere [Hones *et al.*, 1981; Miura, 1995a].

On the other hand, it has been found that wide-band sources, like sudden impulses in the solar wind, produce field-line resonances only at a few  $L$  shells, implying that fast modes of certain frequencies can only exist in the magnetosphere. Therefore it has been suggested that only those fast modes that can get trapped within the magnetospheric cavity between the magnetopause and the plasmapause, can be coupled to shear Alfvén waves, producing field-line resonances [Allan *et al.*, 1986].

In this paper we investigate field-line resonances observed on January 10, 1997. At 21:22 UT, the magnetometer on the IMP 8 satellite located near the bow shock observed a sudden northward turning of the IMF. Then GEOTAIL instruments began to observe fast mode waves and magnetic field vortices in the LLBL/plasma sheet region for several hours. The fast mode waves can trigger field-line resonances on dipole field lines. In fact, POLAR, while moving from the northern polar cap onto dipole field lines, observed field-line resonances at  $L = 10.2$ – $6.6$ .

## Observations

This study presents data from four spacecraft (WIND, IMP 8, GEOTAIL, and POLAR) on January 10, 1997, 21–24 UT. At that time the WIND spacecraft was located in the upstream solar wind at  $(92, -53, -23) R_E$  in GSM. Figure 1 shows the positions of the other spacecraft in the GSM  $xy$  and  $yz$  plane; the bow shock (dashed thin lines) and the magnetopause (solid thin lines) are for the average solar wind conditions (dynamic pressure = 2.1 nPa, IMF  $B_z = 0$ ). All three spacecraft are almost in the dawn-dusk meridian: IMP 8 is in the solar wind (see Figure 1b), GEOTAIL is in the magnetosphere near the LLBL, and POLAR moves from the northern polar cap towards the equator.

We present electric and magnetic field data from POLAR in spacecraft coordinates. Two of the three electric field components are measured with two perpendicular long antennas in the spin plane [Harvey *et al.*, 1995]: the  $xy$  component points radially outward, and the  $z$  component points

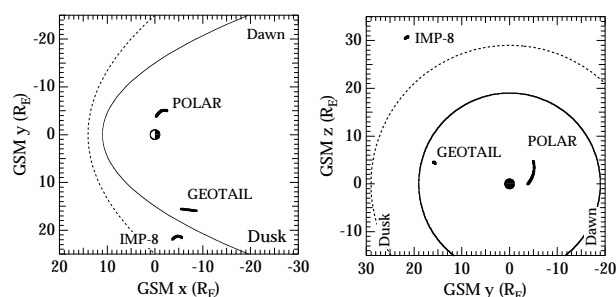


**Figure 1.** Orbits of IMP 8, GEOTAIL, and POLAR in the GSM (a)  $xy$  and (b)  $zy$  planes on January 10, 1997, 21–24 UT.

<sup>1</sup>Finnish Meteorological Institute, Helsinki, Finland.

<sup>2</sup>NASA Goddard Space Flight Center, Greenbelt, MD.

<sup>3</sup>Institute of Geophysics and Planetary Physics, University of California, Los Angeles, CA

<sup>4</sup>Aerospace, Los Angeles, CA

<sup>5</sup>Space Environment Center, NOAA, Boulder, CO.

<sup>6</sup>NASA Space Flight Center, Huntsville, Alabama

<sup>7</sup>Space Sciences Lab., Univ. California, Berkeley, CA.

<sup>8</sup>ISAS, Sagami, Japan.

<sup>9</sup>School of Physics and Astronomy, Univ Minnesota, Minneapolis, MN.

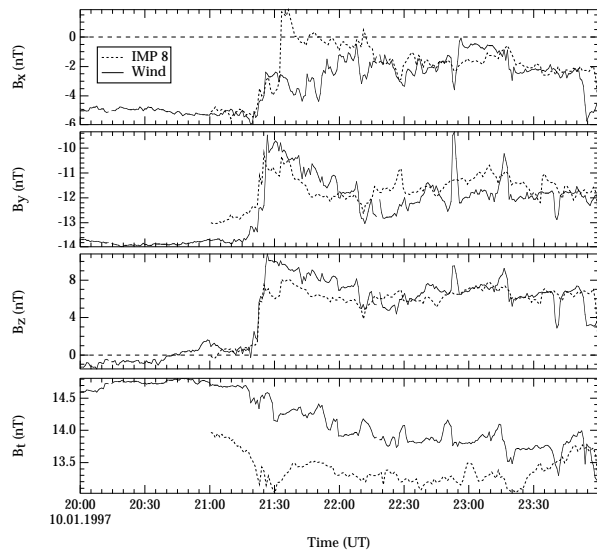


**Figure 2.** Magnetic field observations from the WIND (solid lines) and IMP 8 (dashed lines) spacecraft. The WIND data are shifted forward by 35 minutes.

to the north and is perpendicular to  $xy$ . The third component, measured along the spin axis with a shorter antenna using probes 5 and 6, points into an azimuthal direction and is called 56 (i.e.,  $E_{56}$  and  $B_{56}$ ). The magnetic field, measured at the end of a 6 meter boom, is sampled eight times per second with 11 pT resolution [Russell *et al.*, 1995].

### Solar wind observations

WIND observed a rapid northward IMF rotation at 20:47 UT, and IMP 8 detected this event 35-min later at 21:22 UT. The IMF data are shown in Figure 2, where the WIND data (solid lines) are shifted forward by 35 minutes. At both satellites, the IMF  $B_z$  suddenly increased from a few nT to 10 nT without any significant change in the IMF magnitude. The solar wind speed is about  $430 \text{ km s}^{-1}$  and the distance between these two spacecraft along the  $x$ -axis is  $98 R_E$ , suggesting a 24-min time delay. The observed delay is obtained if the discontinuity is tilted  $+45^\circ$  in the  $xy$  plane.

### POLAR observations

Figure 3 displays the radial electric field component ( $E_{xy}$ ) and an azimuthal magnetic field component ( $B_{56}$ ) measured by POLAR instruments on January 10, 1997, 21–24 UT,

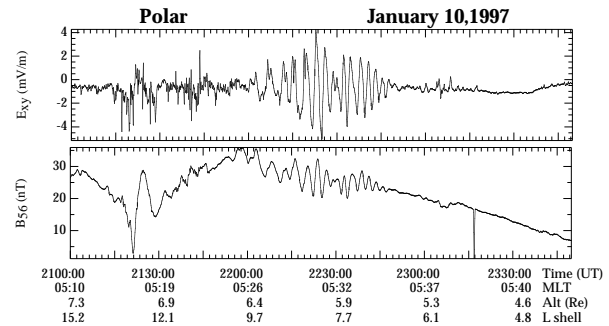


**Figure 3.** Radial electric field component ( $E_{xy}$ ) and azimuthal magnetic field component ( $B_{56}$ ) measured by the POLAR satellite on January 10, 1997, 21–24 UT.

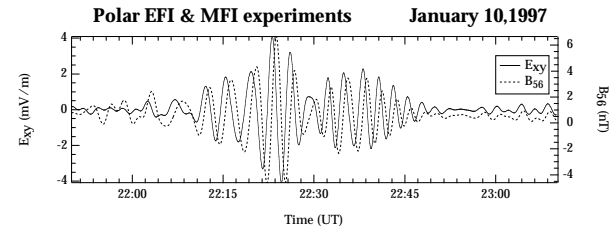


**Figure 4.** Bandpass-filtered time series of  $E_{xy}$  and  $B_{56}$  for the 21:50–23:10 UT interval.

while moving from the northern polar cap toward the equator at 05:30 MLT. At 21:53 UT, POLAR began to observe B-field oscillations whereas E-field oscillations were not observed before 22:10 UT presumably due to the unfavorable orientation of the E-field long booms. The B-field perturbations appear mainly in the azimuthal direction ( $B_{56}$ ), and the electric field oscillates in the radial direction ( $E_{xy}$ ); wave signals in other components are weak. The background magnetic field is oriented along the  $z$ -axis, and therefore we conclude the observed wave is a toroidal mode. Both components are observed at  $L$  shells from 9.0 to 6.6. The observed wave periods vary in the 150–250 s range, corresponding to wave frequencies of 4–7 mHz.

Figure 4 presents bandpass-filtered time series data for the 21:50–23:10 UT interval. Here we have used a Butterworth band-pass filter at  $5 \pm 2$  mHz to remove noise from the data shown in Figure 3. The E- and B-field components are clearly  $90^\circ$  out of phase, indicating that the observed mode is a standing wave.

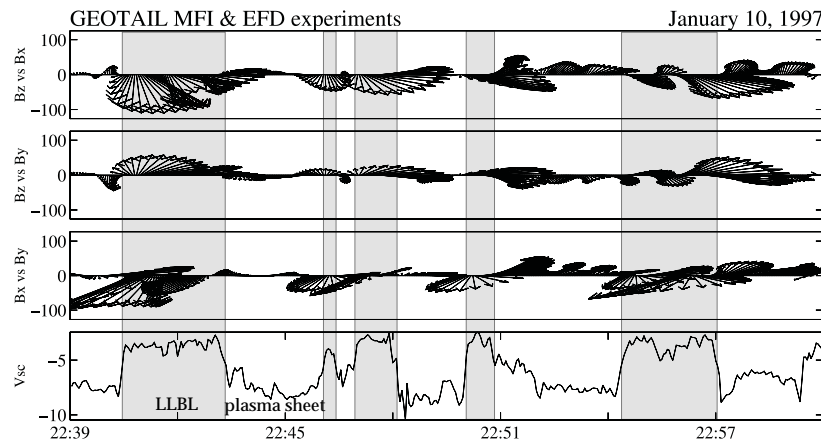


**Figure 5.** Magnetic field and  $V_{sc}$  observations from GEOTAIL at 22:39–23:00 UT. During the shaded intervals the spacecraft was in the LLBL; at the other times it was in the plasma sheet.

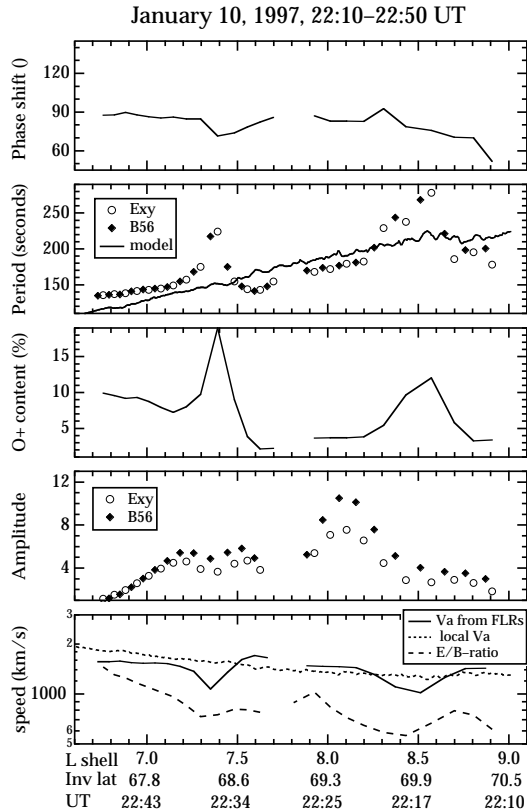


**Figure 6.** Wave characteristics as a function of the satellite's  $L$  shell. See the text for details.

### GEOTAIL observations

During the IMF rotation, GEOTAIL was in the duskside magnetosphere. At 21:28 UT, GEOTAIL suddenly moved into a denser plasma environment, most probably the LLBL. Afterwards, oscillatory perturbations appear in many variables, which persist over several hours.

Figure 5 shows an example of GEOTAIL data for the interval of 22:39–23:00 UT. The bottom panel shows the potential difference  $V_{sc}$  between an electric field probe and the satellite which is related to the ambient electron density [Laakso and Pedersen, 1997]; the more negative  $V_{sc}$ , the lower the density. When  $V_{sc} < -5$  volts, the spacecraft is well inside the magnetosphere, whereas it is in the magnetosheath when  $V_{sc} \geq -2$  volts. When  $V_{sc}$  is between these two regimes, the spacecraft is usually in the LLBL. Therefore the observed  $V_{sc}$ 's suggest that during 21:30–24:00 UT, GEOTAIL encountered the magnetopause a few times,

otherwise the spacecraft was either in the LLBL or in the plasma sheet, as illustrated in Figure 5. The top three panels in Figure 5 show magnetic field vectors in three planes, indicating that magnetic field perturbations are dominated by large-scale vortices, particularly whenever the spacecraft is in the LLBL. In the plasma sheet, both magnetic field vortices and compressional waves were observed. The strongest signals were observed at 1–15 mHz.

The total magnetic field  $B_t$  and  $V_{sc}$  (i.e., the electron density) are well correlated so that large  $B_t$ 's occur at large densities. Figure 6 shows the power spectral densities of  $V_{sc}$  (solid line) and  $B_t$  (dashed line) at 1–20 mHz for the 22:05–22:56 UT interval. A good correlation between these two variables suggests that the fluctuations are compressional perturbations; possible sources are surface waves moving the spacecraft between two plasma regions and fast mode waves generated by the K-H instability. Lowest frequencies in Figure 6 are related to surface waves and are in agreement with the power spectra of ULF waves observed with the high-latitude ground-based magnetometers [Clauer *et al.*, 1997].

### Discussion

A rapid northward IMF turning produced a variety of magnetospheric processes on January 10, 1997. This rotation was followed by the formation of surface waves in the magnetopause/LLBL region via the K-H instability, resulting in the motion of GEOTAIL between two plasma regions, mainly between the plasma sheet and the LLBL. In the LLBL, large-scale magnetic field vortices were observed, whereas in the plasma sheet both vortices and fast mode waves were observed. The strongest compressional waves occurred at 1–15 mHz whereas the field-line resonances observed by POLAR occurred at 4–7 mHz. One open question is how a broad-band source produces only resonances with a narrow-band frequency range (see e.g., Allan *et al.* [1986]).

Figure 6 presents wave characteristics of the field-line resonances as a function of POLAR's  $L$  shell. The panels from top to bottom are: phase difference between  $B_{56}$  and  $E_{xy}$  (positive values mean that E-field leads B-field), oscillation periods  $T_{obs}$ , oxygen content, peak-to-peak amplitudes, and velocities. The phase difference between  $E_{xy}$  and  $B_{56}$  is near  $90^\circ$ , indicating that observed waves are standing modes.

$T_{obs}$ , derived from E- and B-field measurements (diamonds -  $B_{56}$ , circles -  $E_{xy}$ ), are in good agreement with each other and tend to increase with  $L$  shell, indicating that different  $L$  shells oscillate independently. At  $L = 7.4$  and  $8.5$ ,  $T_{obs}$  has peaks that deviate from the trend over the inter-

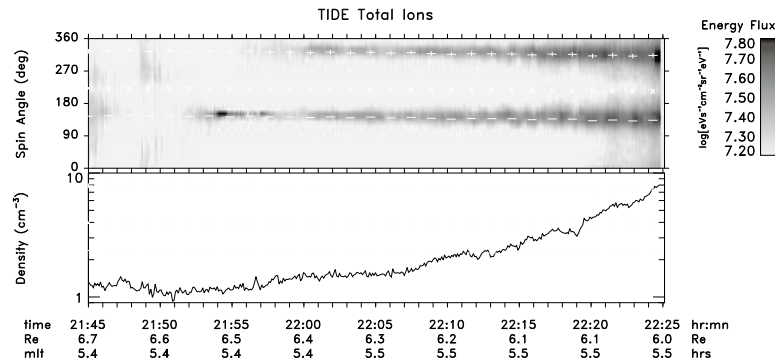


**Figure 7.** Energy fluxes of ions (top panel) and the total ion density (bottom panel). Enhanced fluxes occur parallel (indicated + signs) and antiparallel (– signs) to the field lines.

val. The solid line represents the model oscillation period,  $T_{mod}$ , of the fundamental mode of the field-line resonance of dipole field lines;  $T_{mod}$  is based on the local Alfvén speed  $V_A$  at POLAR, and on the assumptions that 5% of the ions are oxygen ions and  $V_A$  is constant along each dipole field line. The electron density is derived from the spacecraft potential measurements. The differences between  $T_{obs}$  and  $T_{mod}$  suggest that there are more heavy ions on the field-lines where  $T_{obs}$  has peaks. The third panel in Figure 6 shows the  $O^+$  number density, assuming that  $T_{obs}$  and  $T_{mod}$  match. According to this result, the background  $O^+$  density is usually a few percent, but some field lines are filled with higher  $O^+$  densities.

The TIDE detector is turned off below about  $L = 8$ , but before that starting at 21:53 UT, it detected 5-10 eV ions streaming outward from the ionosphere along the magnetic field (see Figure 7). Note that ions flowing parallel to the field lines are observed later because they need to propagate from the southern hemisphere to the northern one. This suggests that the ion outflow has been initiated by field-line resonances. Unfortunately the ion masses cannot be determined. Therefore the predicted peaks in  $O^+$  density cannot be confirmed with TIDE. On the other hand, the TIMAS instrument on POLAR, which measures ions with energy greater than 15 eV, shows no enhancements in the  $O^+$  density (Bill Peterson, private communication, 1997). The explanation may be that the energies of the outflowing heavy ions are below 15 eV or high  $O^+$  densities exist at lower altitudes because of their lower speeds.

The fourth panel from the top in Figure 6 shows the wave amplitudes for  $E_{xy}$  and  $B_{56}$  (units are  $mV m^{-1}$  and  $nT$ , respectively), which both are peaked at 7.4 (68.2° inv. lat.) and 8.1 (69.2° inv lat). It seems that oscillation periods and wave amplitudes are somewhat anticorrelated so that high  $O^+$  densities tend to reduce wave amplitudes.

In the bottom panel of Figure 6 the dashed line represents the  $E_{xy}/B_{56}$  ratio. The solid line represents the average  $V_A$  along field lines, derived from  $T_{obs}$  of the field line resonances. The dotted line represents the local  $V_A$  on POLAR, using the electron densities derived from the spacecraft potential measurements, and assuming a 5%  $O^+$  number density. The measured  $E_{xy}/B_{56}$  is related to  $V_A$ , as expected; notice that these parameters have been derived from different data. The actual difference between these two parameters is not significant, because the  $E_{xy}/B_{56}$  ratio varies along the field line so that at magnetic field nodes it approaches infinity, and at electric field nodes it goes to zero.

## Summary

A sudden northward rotation of the IMF was observed by IMP 8 near the bow shock at 21:22 UT on Jan 10, 1997, coincided with the formation of the K-H instability at the magnetopause/LLBL layer. GEOTAIL located in these region moved between the LLBL and the plasma sheet as a result of the surface waves. During this time, its instruments detected magnetic field vortices and fast mode waves. The fast mode waves have much broader power spectra than the narrow-banded field-line resonances simultaneously observed by POLAR at  $L = 10.2$ -6.6. The ULF waves are a likely candidate to produce ion outflow from the ionosphere. In addition, the field-line resonances show two unexpected peaks in the oscillation periods which can be explained with  $O^+$ -rich field lines.

**Acknowledgments.** We wish to thank S. Kokubun for the use of the GEOTAIL magnetic field data. H.S. was supported in part by NASA Interagency Order No. S-67019-F. H.L. was supported in part by an ISTP grant to the POLAR/EFI team at GSFC.

## References

- Allan, W. et al., Hydromagnetic wave coupling in the magnetosphere - plasmapause effects on impulse-excited resonances, *Planet. Space Sci.*, 34, 1189-1200, 1986.
- Clauer, C.R. et al., Field line resonant pulsations associated with a strong dayside ionospheric shear convection flow reversal, *J. Geophys. Res.*, 102, 4585-4596, 1997.
- Harvey, P. et al., The electric field instrument on the Polar satellite, *Space Sci. Rev.*, 71, 583-596, 1995.
- Hones, E. W., Jr. et al., Further determination of the characteristics of magnetospheric plasma vortices with Isee 1 and 2, *J. Geophys. Res.*, 86, 814-820, 1981.
- Hughes, W. J., Magnetospheric ULF waves: A tutorial with a historical perspective, in *Solar Wind Sources of Magnetospheric Ultra-Low-Frequency Waves*, edited by M. J. Engebretson et al., Monograph 81, pp. 1-11, AGU, 1994.
- Laakso, H. and A. Pedersen, Ambient electron density derived from differential potential measurements, in *Measurement Techniques*, edited by J. Borovsky, R. Pfaff, and Young, AGU Monograph, in press, 1997.
- Laakso, H. and R. Schmidt, Pc 4-5 pulsations in the electric field at geosynchronous orbit (GEOS 2) triggered by sudden storm commencements, *J. Geophys. Res.*, 94, 6626-6632, 1989.
- Miura, A., K-H instability at the magnetopause: computer simulations, in *Physics of the Magnetopause*, edit. P. Song et al., AGU Monog. 90, 285-291, 1995a.
- Miura, A., Dependence of the magnetopause K-H instability on the orientation of the magnetosheath magnetic field, *Geophys. Res. Lett.*, 22, 2993-2996, 1995b.
- Pu, Z-Y, and M. G. Kivelson, Kelvin-Helmholtz instability at the magnetopause: energy flux into the magnetosphere, *J. Geophys. Res.*, 88, 853-861, 1983.
- Russell, C. T. et al., The GGS/POLAR magnetic fields investigation, *Space Sci. Rev.*, 71, 563-582, 1995.
- Samson, J. C., J. A. Jacobs, and G. Rostoker, Latitude dependent characteristics of long-period geomagnetic micropulsations, *J. Geophys. Res.*, 76, 3675-3683, 1971.
- Singer, H. J., W. J. Hughes, and C. T. Russell, Standing hydromagnetic waves observed by ISEE 1 and 2: radial extent and harmonic, *J. Geophys. Res.*, 87, 3519-, 1982.
- Southwood, D. J., Some features of field line resonances in the magnetosphere, *Planet. Space Sci.*, 22, 483-491, 1974.
- J. Clemmons, Aerospace, Los Angeles, CA.
- D. H. Fairfield, R. P. Lepping, R. F. Pfaff, Code 690, NASA Goddard Space Flight Center, Greenbelt, MD 20771.
- B. L. Giles, Space Science Laboratory, NASA Space Flight Center, Huntsville, Alabama 35812.
- H. Laakso, Finnish Meteorological Institute, Geophysical Research, Helsinki, Finland.(e-mail: harri.laakso@fmi.fi)
- F. S. Mozer, Space Sciences Laboratory, University of California, Berkeley, CA 94720-7450.
- C. T. Russell, Institute of Geophysics and Planetary Physics, University of California, Los Angeles, CA 90095.
- H. J. Singer, Space Environment Center, NOAA R/E/SE, 325 Broadway, Boulder, CO 80303.
- K. Tsuruda, Institute of Space and Astronautical Science, Yoshinodai, Sagami-hara, Kanagawa 299, Japan.
- J. R. Wygant, School of Physics and Astronomy, University of Minnesota, Minneapolis, MN 55455.

(Received October 16, 1997; revised January 5, 1998; accepted February 4, 1998.)